Acta Cryst. (1969). A**25**, 589

X-ray Study of Diffuse Streak Diffraction Pattern from Silicon Single Crystals

BY A. BONEFAČIĆ*

Laboratoire de Physique des Solides, Faculté des Sciences, 91 *Orsay, France*

(*Received* 19 *February* 1969 *and in revised form* 1 *April* 1969)

Diffuse X-ray scattering by silicon single crystals has been detected on the film by the use of a doubly bent crystal monochromator. The intensities of one diffuse streak were measured at 83°K and 273°K with a scintillation counter spectrometer. With rising temperature the intensity of the diffuse streaks was increased, confirming their thermal origin. In order to examine the scattering in detail, measurements of the absolute thermal scattering power were made through a large region of the ($\bar{1}01$) reciprocal lattice plane at 293°K. These measurements were compared with the theoretical values of the thermal scattering power, given by the theory developed by Laval, in which temperature vibrations are expressed in terms of elastic waves. The first-order term only was calculated and higher-order terms were neglected. The measurements are in semi-quantitative agreement with this theory.

Introduction

A characteristic streak X-ray diffraction pattern from silicon single crystals was first noticed by Kodera, Kitamura & Honjo (1963) in a photograph taken with filtered Mo radiation parallel to the [100] axis. This characteristic type of diffuse scattering has also been seen in electron diffraction diagrams, as well as in X-ray diagrams on some other substances. Honjo, Kodera & Kitamura (1964) inferred that the streak patterns by silicon single crystals indicate a predominant clustered motion of linear scatterers along ⟨110⟩ directions, the scatterers consisting of zigzag chains of the nearest neighbour silicon atoms. Komatsu (1964) gave a revised interpretation in terms of the dynamical theory of lattice vibrations. He considered transverse acoustic waves, polarized in the direction of the atomic chains, having predominantly low frequencies. This gives a particular intensity distribution restricted to the {110} reciprocal planes, but without diffuse scattering in the reciprocal planes passing through the origin. A quantitative analysis of the intensity distribution of diffuse streaks in silicon single crystals has not yet been given.

Recent X-ray studies of diffuse thermal scattering on silicon single crystals were made by Corbeau (1964) and Banerjee (1967). Their measurements were confined to several special directions in the crystal lattice in order to obtain the dispersion relations of lattice vibrations (Corbeau) or to determine the Compton scattering of silicon crystal (Banerjee, 1967). Dispersion curves in special directions on crystals which have a diamond structure were measured also by Brockhouse & Iyengar (1958) and by Dolling (1962) by means of inelastic neutron scattering. In all these studies no special attention has been given to the streak diffusion pattern in silicon single crystals. The explanation of the origin of the streaks seems to require more systematic experimental and theoretical studies. Thus we decided to make our measurements of scattered X-ray radiation throughout a large region of reciprocal space paying special attention to the ($\bar{1}01$) plane.

Experimental

(a) Recording of diffuse streaks and measurements of their variation with temperature

The silicon single crystal used for the experiment and prepared by careful grinding, polishing and etching was approximately $5 \times 5 \times 0{\cdot}1$ mm³ and cut so that its face was parallel to the (111) planes. X-rays from a well stabilized, full wave rectified copper target tube run at 40 kV and 16 mA were monochromatized by a toroidally bent LiF crystal plate, set to reflect the Cu $K\alpha$ radiation on the (200) planes. The beam was focused on the face of the crystal which was oriented with the axis [111] parallel to the beam. The transmission photographs were obtained both on a plane film and on a cylindical film [Fig. 1(*a*), (*b*)]. Besides Laue spots conspicuous diffuse streaks can be seen in both photographs. Fig. 1(*c*) represents the projection, on the cylinder, of the intersections of the {110} reciprocal planes with the Ewald sphere, which corresponds to the setting of the crystal. The diffuse streaks in Fig. 1(*b*) correspond to the parts of curves indicated by thicker lines in Fig. 1(*c*). Thus it is evident that the diffuse streaks correspond to the intersections of the {110} reciprocal planes with the Ewald sphere.

In order to verify their thermal origin the intensities of one of these streaks, situated in Fig. 1(*b*) between the 111 and 313 reflexions, were measured at 273°K and 83°K by means of a recording scintillation counter spectrometer. The crystal, placed in an evacuated chamber, was mounted on a goniometer head which was in thermal contact with liquid nitrogen. The temperature of the crystal was measured with a thermocouple fastened to the support of the crystal.

The intensities obtained are represented in Fig. 2. The full curve and the dashed curve represent the results of the measurements at 83°K and 293°K respec-

* Present address: Institute of Physics of the University of Zagreb, Yugoslavia.

tively. An eight-second counting interval only was used to avoid the formation of ice on the silicon surface during the measurements. Thus the deviations of the measured points from the smoothed curves are considerable.

(*b*) *Measurements of the absolute magnitude of the thermal scattering*

The measurements of the absolute magnitude of the thermal diffuse scattering were made at room temperature. X-ray data and the method of monochromatization were the same as in (*a*). The crystal used was a single crystal with dimensions $15 \times 15 \times 4$ mm^3 cut so that its face was parallel to the (111) planes. After polishing and etching, the crystal was placed in an evacuated chamber. The reflected intensities were detected with a scintillation counter (NaI crystal activated with Tl). The measurements of the diffuse reflexions were carried out by placing the crystal and the detector in such a position that the measurements could be done in the direction [111] of the reciprocal lattice from $2\sin\theta/\lambda = 0{\cdot}358.10^8$ to $0{\cdot}917.10^8$, as well as in 19 additional directions, in the $(\bar{1}01)$ reciprocal plane, which varied in steps of two degrees on both sides of the [111] direction, as visible from Table 1 and Fig. 3. The intensity of the direct beam was evaluated at the beginning and at the end of the measurements of the intensities of scattered radiation corresponding to a given direction. A three-minute counting interval was used in the measurements of the scattered radiation and ten three-minute measurements were made for each evaluation of the direct beam. This made it possible to explore the part of the $(\bar{1}01)$ reciprocal plane lying between 111, 131, 313 and 333 reciprocal lattice points (relps). The setting and the recording were made automatically. The readings obtained from the scaler were automatically recorded by means of a print-out unit which converted the readings of the scaler into numbers. The harmonics of the characteristic radiation could not be completely eliminated with the discriminator only. Therefore an aluminum filter was used to estimate the intensities of the half-wavelength reflected by the monochromator. The fluctuation of the scattered radiation flux printed out was less than 3%. This flux, $i(\mathbf{X})$, is related to the diffuse scattering power $\mathscr{I}(\mathbf{X})$ in the relation given by Guinier (1964). $\mathscr{I}(\mathbf{X})$, modified to express the scattering relating to an electron of the crystal, may be written as follows:

$$\mathscr{I}(\mathbf{X}) = \frac{i(\mathbf{X})\mu \, . \, \varrho(1+\sin\alpha/\sin\beta)v_1(1+\cos^2 2\alpha')}{7{\cdot}90 \, . \, 10^{-26}\varepsilon E_0(1+\cos^2 2\alpha' \cos^2 2\theta)\mathrm{d}\omega} \quad (1)$$

where the symbols have the following meanings:

$\mathbf{X}$ vector of diffuse scattering. $|\mathbf{X}| = 2\sin\theta/\lambda$;
μ mass absorption coefficient of the sample (60·6 cm^{2}g^{-1});
ϱ density of the sample (2·4 g.cm^{-3});
α and β angles of incidence and of diffuse reflexion of X-rays on the silicon crystal;
α' angle of reflexion on the monochromator;
v_1 volume of the unit cell ($160{\cdot}19 \, . \, 10^{-24}$ cm^3);
ε number of electrons in a unit cell;
E_0 total flux of the incident X-ray beam;
$\mathrm{d}\omega$ solid angle of X-rays entering the counter ($1{\cdot}07 \times 10^{-3}$ sterad);
2θ angle of diffuse scattering.

The ratio $i(\mathbf{X})/E_0$, in (1), was obtained experimentally by dividing the measured flux of the diffusely reflected radiation by that of the incident radiation. It was obtained as the ratio between the number of counts,

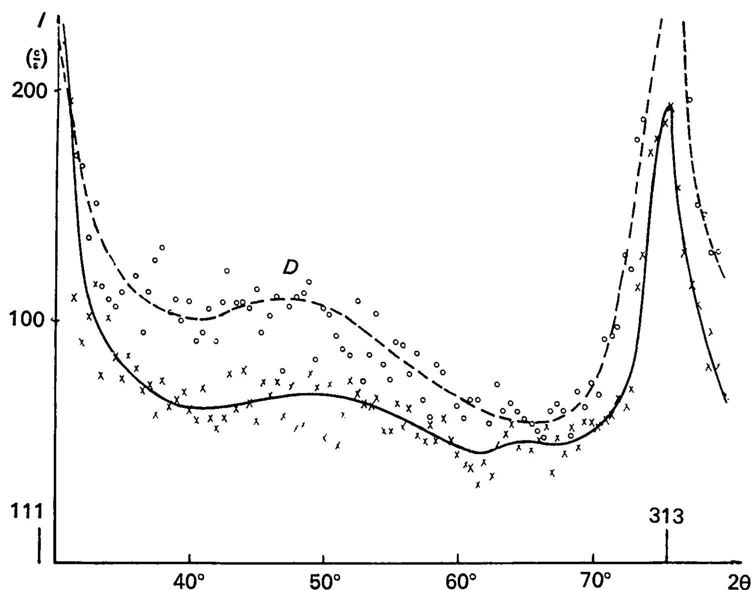

Fig. 2. Measured relative intensities between (111) and (313) relps, at 83 °K (full curve) and 293 °K (dashed curve). The maximum marked with *D* belongs to the diffuse streak.

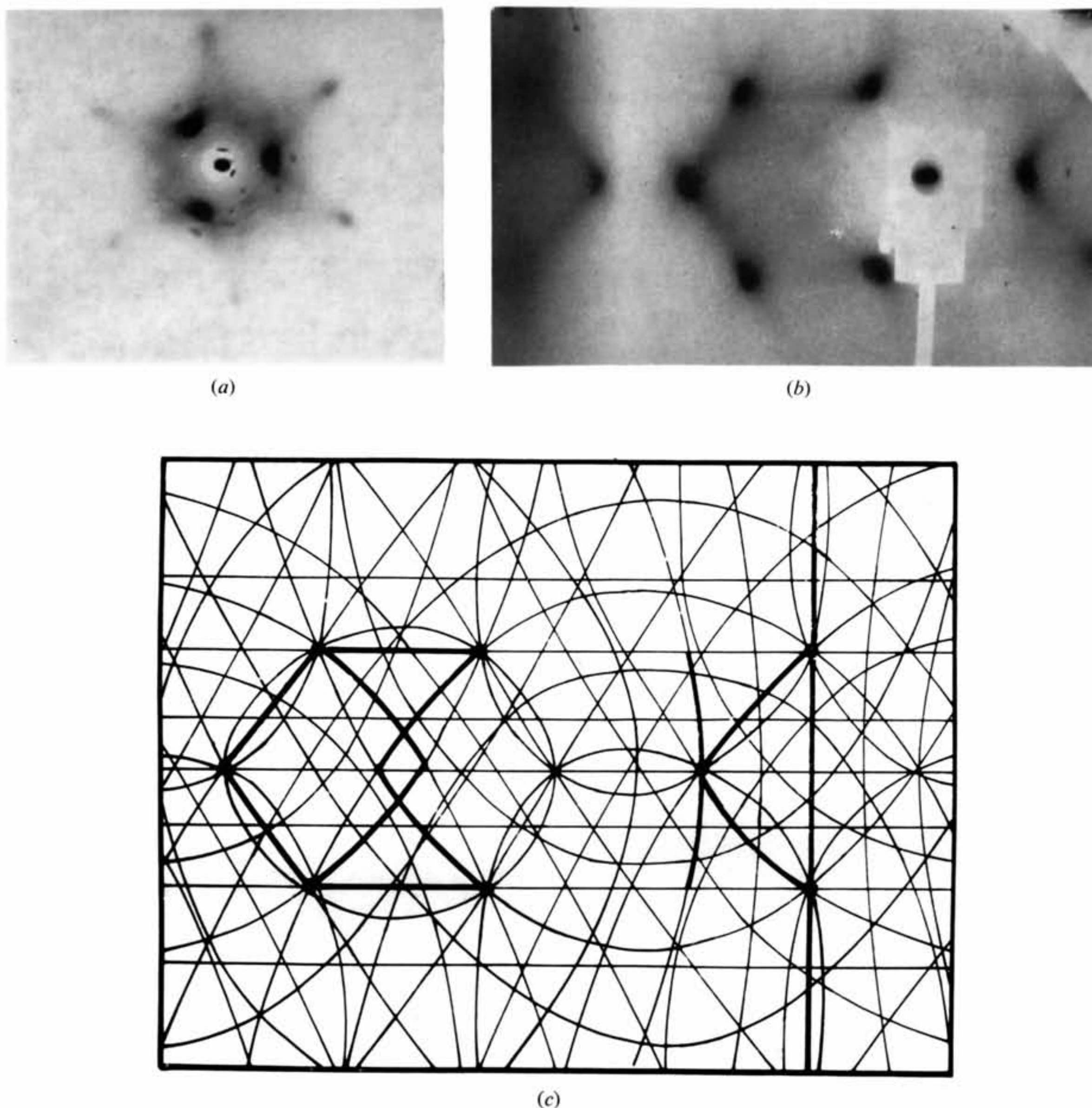

(a) (b) (c)

Fig. 1. (a) Stationary crystal X-ray transmission photograph on a plane film. The photograph is taken with Cu radiation monochromatized by a toroidally bent LiF crystal plate, set to reflect the Cu $K\alpha$ radiation on the (200) planes. The silicon single crystal was oriented with the [111] axis parallel to the beam. Exposure time: 5 hours. (b) Same as (a) but photographed on a cylindrical film. [$\bar{1}$01] axis parallel to the cylinder axis. (c) The curves represent the projection on the cylinder of the intersections of the {110} reciprocal planes with the Ewald sphere. ⟨111⟩ axis parallel to the beam, ⟨110⟩ parallel to the chamber axis.

recorded in unit time, when the diffuse radiation is entering the detector, and the number of counts in unit time when the whole of the direct beam is allowed to enter the detector. This ratio being small (about 10^{-7}), it was necessary to reduce the flux of the direct beam by carefully calibrated nickel foils.

The measurements being made far enough from the relps, divergence corrections could be neglected. From the diffuse scattering power calculated by (1), the Compton modified component, given by Freeman (1959), was subtracted and the remainder treated as the thermal diffuse scattering $I(\mathbf{X})$. The results are given in Table 1 and shown in Fig. 4(*a*) in the form of a contour plot of equidiffusion lines.

Calculation of the first-order thermal diffuse scattering power

Following Laval (1954) the first-order thermal scattering power P, relating to the scattering of an electron of the crystal, is given by

$$P=\frac{|\mathbf{X}|^2}{\varepsilon m}\sum_{\gamma=1}^{6}\left(\frac{W}{\nu^2}\right)_{S_\gamma}|\Phi_{S_\gamma}|^2 .$$

The new symbols have the following meanings:

m mass of the unit cell;

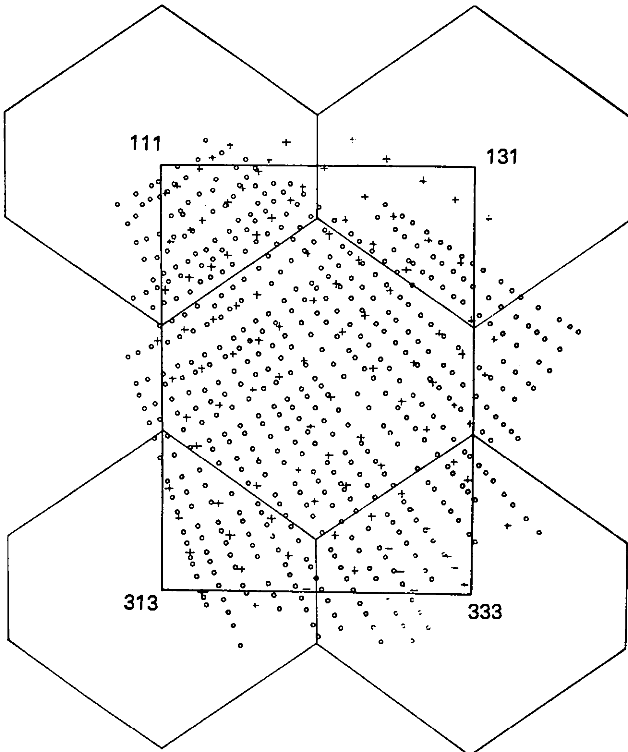

Fig. 3. The ($\bar{1}01$) plane of a reciprocal lattice of silicon, each lattice surrounded by its own zone. Small circles indicate the points of measurements of scattered intensities, and crosses the points in which the first-order thermal scattering power was calculated.

$$\left(\frac{W}{\nu^2}\right)_{S_\gamma}=\frac{h}{\nu_{S_\gamma}}\left[\frac{1}{\left(\exp\frac{h\nu_{S_\gamma}}{kT}\right)-1}+\tfrac{1}{2}\right];$$

h Planck's constant;

k Boltzmann's constant;

T temperature;

ν_{S_γ} frequency of the oscillation S_γ, **S** being the wave vector;

$$\Phi_{S_\gamma}=\sum_j f'_j \chi^j_{S_\gamma}\exp\left[i2\pi(\mathbf{Mj}+\varphi^j_{S_\gamma})\right];$$

f'_j atomic structure factor f_j, multiplied by the Debye–Waller factor H_j;

M vector of the lattice translation;

j average position of the jth atom in the unit cell;

$$X^j_{S_\gamma}=\frac{1}{|\mathbf{X}|}\left(\frac{m}{m_j}\right)^{1/2}\left|\sum_\alpha X_\alpha \varrho^j_{\alpha S_\gamma}\exp\left(i2\pi\varphi^j_{\alpha S_\gamma}\right)\right|;\ (\alpha=1,2,3)$$

m_j mass of the jth atom;

$\varrho^j_{\alpha S_\gamma}$, represents modulus and $2\pi\varphi^j_{\alpha S_\gamma}$ phase of $\zeta^j_{\alpha S_\gamma}$ defined by

$$\zeta^j_{\alpha S_\gamma}=\varrho^j_{\alpha S_\gamma}\exp\left[-i2\pi(\mathbf{Sj}-\varphi^j_{\alpha S_\gamma})\right].$$

$\varrho^j_{\alpha S\gamma}$ are the components of the proper vectors of the dynamical matrix (Fourier matrix). For the diamond lattice type, to which the silicon lattice belongs, the form of the matrix was determined by Smith (1948). Generally, the form of this matrix is as follows:

$$\begin{bmatrix} F & J & K & A & B & C\\ J & G & L & B & A & E\\ K & L & H & C & E & A\\ A^* & B^* & C^* & F & J & K\\ B^* & A^* & E^* & J & G & L\\ C^* & E^* & A^* & K & L & H \end{bmatrix} \quad (3)$$

The approximation to the frequency distribution is obtained by considering the second-neighbour force as central. Then:

$$F=4[\alpha+\mu\{2-\cos(\pi S_x)\cos(\pi S_y)-\cos(\pi S_z)\cos(\pi S_x)\}]$$
$$J=4\mu\sin(\pi S_x)\sin(\pi S_y)$$
$$K=4\mu\sin(\pi S_z)\sin(\pi S_x)$$
$$L=4\mu\sin(\pi S_y)\sin(\pi S_z)$$
$$G=4[\alpha+\mu\{2-\cos(\pi S_y)\cos(\pi S_z)-\cos(\pi S_x)\cos(\pi S_y)\}]$$
$$A=-\alpha[1+\exp\{-\pi i(S_x+S_y)\}+\exp\{-\pi i(S_z+S_x)\}+\exp\{-\pi i(S_y+S_z)\}]$$
$$B=-\beta[1+\exp\{-\pi i(S_x+S_y)\}-\exp\{-\pi i(S_z+S_x)\}-\exp\{-\pi i(S_y+S_z)\}]$$
$$C=-\beta[1-\exp\{-\pi i(S_x+S_y)\}+\exp\{-\pi i(S_z+S_x)\}-\exp\{-\pi i(S_y+S_z)\}]$$

$$E = -\beta[1 - \exp\{-\pi i(S_x+S_y)\} - \exp\{-\pi i(S_z+S_x)\} + \exp\{-\pi i(S_y+S_z)\}]$$
$$H = 4[\alpha+\mu\{2-\cos(\pi S_z)\cos(\pi S_x) - \cos(\pi S_y)\cos(\pi S_z)\}] .$$

In these equations S_x, S_y and S_z are the components of the wave vector **S**. In order to simplify the calculation, we divided the range of 0 to 1 of S_x, S_y and S_z in the first Brillouin zone into eighths, introducing the vector components

$$S_i = P_i/8$$

where $i = x,y,z$ and P_x, P_y, P_z are integers from 0 to 8. The constants α, β and μ are derived from the elastic constants c_{11}, c_{12} and c_{44} measured by McSkimin (1953) at 293°K,

$$c_{11} = 1{\cdot}674 \,.\, 10^{12} \text{ dyne.cm}^{-2}$$
$$c_{12} = 0{\cdot}652 \,.\, 10^{12} \text{ dyne.cm}^{-2}$$
$$c_{44} = 0{\cdot}796 \,.\, 10^{12} \text{ dyne.cm}^{-2}$$

and from the value of the fundamental frequency of silicon found by Corbeau (1963) ($\nu_0 = 15{\cdot}7 \,.\, 10^{12}$ s^{-1}). Thus we obtain:

$$\alpha = 5{\cdot}35 \,.\, 10^4 \text{ dyne.cm}^{-1},$$
$$\beta = 3{\cdot}83 \,.\, 10^4 \text{ dyne.cm}^{-1},$$
$$\mu = 0{\cdot}171 \,.\, 10^4 \text{ dyne.cm}^{-1}.$$

In spite of the approximation, the matrix (3) has no general solution and must be solved numerically. In order to determine the frequency distribution, the roots of the characteristic equation

$$[\omega^2 I - \Gamma] = 0 \qquad (4)$$

were calculated. In this equation $\omega = 2\pi\nu$, I is the unit matrix of order $3g \times 3g$, g being the number of atoms in a unit cell and Γ represents the dynamical matrix in reciprocal space. The frequency distribution is calculated for a set of integers (P_x, P_y and P_z) which correspond to the following directions of the wave vector in the first Brillouin zone: [010], [171], [151], [272], [131], [121], [533], [111], [212], [313], [515] and [101].

The dispersion curves of elastic waves as well as the first-order thermal diffuse scattering power were calculated on a UNIVAC 1107 machine. The first-order thermal diffuse scattering power was calculated at points shown in Fig. 3. The results obtained are given in Table 2. On the basis of these values a contour plot of equidiffusion lines in the reciprocal space is made as shown in Fig. 4(*b*).

Results and discussion

From the appearance of the curves in Fig. 2 it may be concluded that the intensity of the diffuse streak

Table 1. *Measured values of the thermal diffuse scattering power* $I(|\mathbf{X}|) \,.\, 10^3$

$\|X\| . 10^{-8}$	Directions																			
	[111]+20°	[111]+18°	[111]+16°	[111]+14°	[111]+12°	[111]+8°	[111]+6°	[111]+4°	[111]+2°	[111]	[111]−2°	[111]−4°	[111]−6°	[111]−8°	[111]−10°	[111]−12°	[111]−14°	[111]−16°	[111]−18°	[111]−20°
0.336					604	922			1054		941				229					
0.357					450	632	524	507	487	407	389	402	395		288					
0.379					357	415	359	328	256	257	247	267	265		281	214				
0.401					306	344	281	261	196	208	197	212	220	235	238	209				
0.422					199	306	246	240	189	184	175	168	191	200	218	202				
0.444			392	262	220	268	247	223	174	145	147	130	164	172	202	157	147			
0.464			271	260	190	262	244	217	151	119	127	106	145	150	182	155	151			
0.486			257	237	180	261	224	218	138	108	120	93	136	153	168	153	150			
0.507	339	390	309	245	190	222	218	216	133	95	112	90	130	144	160	146	149			
0.527	330	388	352	259	214	225	213	211	128	85	110	97	125	137	160	152	154			
0.548	396	441	385	299	247	272	225	214	133	92	123	104	125	153	179	172	179	200	196	127
0.569	335	382	362	282	232	275	231	215	130	92	119	104	125	154	189	179	197	235	271	262
0.589	242	289	289	229	191	265	221	211	126	100	115	102	120	158	197	162	206	269	287	330
0.609	189	230	225	170	147	228	228	192	125	139	126	110	127	114	197	124	200	243	284	312
0.629	150	184	165	136	117	181	199	194	116	794	128	109	127	146	144	104	165	165	208	218
0.649	137	227	155	135	131	175	194	189	123	731	138	120	134	127	132	108	128	137	155	176
0.668	143	170	143	144	146	217	248	197	123	191	139	129	134	128	132	122	86	125	137	147
0.687	142	187	153	187	193	263	289	222	147	132	151	139	170	162	159	155	88	126	142	164
0.706	159	217	187	249	248	253	271	246	163	127	149	144	181	179	182	191	150	126	150	166
0.725	212	280	284	317	282	268	271	246	175	146	163	161	178	212	234	250	182	162	167	182
0.744	310	398	367	358	295	296	269	273	171	160	167	173	193	231	257	304	212	191	188	206
0.762	568	623	507	397	312	334	314	262	188	182	219	207	213	259	294	344	315	233	226	242
0.781	1256	844	645	434	340	370	343	293	203	190	192	233	214	253	319	360	321	285	264	285
0.799	2255	1127	705	557	429	440	379	357	229	217	215	299	247	304	345	417	447	383	329	314
0.816	2054	1229	895	691	539	509	431	384	261	236	230	337	282	331	375	489	534	512	539	463
0.834	1090	1005	890	801	695	603	537	422	305	266	266	379	334	354	439		662	668	628	672
0.851		662	658	715	731	713	602	481	363	300	296	410	383		506					
0.868		415	514	595	658	842	749	557	433	355	349	443	478		672					
0.885		360			529	840	919	696	549	473	447	526	653		886					
0.901		300			431	757	896	977	750	647	621		827		1182					
0.917		283			353	650	815	1083	1196		858		820							
0.933						544	724	1114					890							
0.949						453	654	1131					744							
0.965							624	1082												

(marked with D) diminishes as the temperature falls from 293 °K to 83 °K. Thus the temperature dependence of the intensity of the diffuse streak proves the thermal origin of the streak. At the same time spot 111 becomes stronger and spot 313 weaker. It is possible that the thermal expansion of the crystal moved relp 111 nearer to the Ewald sphere and 313 further from it, thus causing the observed changes in intensity.

Fig. 4(a) represents a contour plot of the measured power of thermal diffuse scattering at 293 °K, which was obtained by subtracting the Compton modified scattering, calculated by Freeman (1959), from the measured diffuse scattering. The occurrence of a comparatively strong 'forbidden' maximum in relp 222 is explained by Renninger (1937) and Heidenreich (1950) on the basis of the dynamical theory and is to be expected in diamond structures. This maximum influences the aspect of the equidiffusion contours obtained by measurements, but does not exist in the calculated contour plot represented in Fig. 4(b). Experimentally a quantitatively stronger diffusion streak was found than by calculation. A better fit would probably be attained with a more rigorous calculation of the vibration frequencies, without the approximation of the frequency distribution. Uncertainties exist also in the determination of the Compton modified scattering. In some recent articles on the Compton effect, Banerjee (1964, 1967) describes anomalies in the values of the intensities of scattered radiation. However, in both Fig. 4(a) and Fig. 4(b) the diffuse streak between 313 and 333 relps is evident. Moreover, the calculated streaks are about equally widespread as those experimentally observed. Thus we may conclude that thermal diffuse scattering is concentrated in the {110} reciprocal lattice planes, the greatest intensity appearing between relps, and that the diffuse streak diffraction patterns from silicon single crystals may be explained in terms of thermal scattering.

It is interesting to make a comparison between the diffuse scattering pattern of silicon and those observed in diamonds and barium titanate. In the case of diamonds the extra X-ray reflexions are two of kinds. One, dependent upon temperature and identified with thermal diffuse scattering, and another largely independent

Table 2. *Calculated values of the first-order thermal diffuse scattering power P*

Direction	$X = \frac{2 \sin \theta}{\lambda} \cdot 10^{-8}$	P
[2 5 2]	0.454	0.211
	0.517	0.356
	0.558	0.398
	0.599	1.341
	0.629	0.168
[1 2 1]	0.401	0.183
	0.454	0.226
	0.517	0.204
	0.558	0.156
	0.599	0.090
	0.629	0.050
[3 5 3]	0.401	0.194
	0.454	0.227
	0.517	0.192
	0.558	0.136
	0.599	0.065
	0.697	0.116
	0.744	0.144
[2 3 2]	0.358	0.173
	0.401	0.244
	0.454	0.229
	0.517	0.211
	0.558	0.115
	0.599	0.021
	0.697	0.061
	0.744	0.189
[3 4 3]	0.358	0.338
	0.401	0.272
	0.454	0.216
	0.517	0.211
	0.558	0.157
	0.599	0.070
	0.668	0.087
	0.697	0.106
	0.744	0.187
	0.799	0.336
[5 6 5]	0.358	0.493
	0.401	0.282
	0.454	0.271
	0.558	0.154
	0.599	0.067
	0.668	0.032
	0.697	0.133
	0.744	0.205
	0.799	0.311
	0.834	0.468
	0.876	0.473
[5 2 5]	0.629	0.014
	0.668	0.015
	0.697	0.029
	0.744	0.132
	0.799	1.248
[1 1 1]	0.358	0.521
	0.401	0.286
	0.454	0.221
	0.517	0.141
	0.558	0.118
	0.599	0.085
	0.668	0.101
	0.706	0.157
	0.744	0.209
	0.834	0.354
	0.876	0.516
	0.917	1.091
[7 6 7]	0.358	0.374
	0.401	0.307
	0.454	0.220
	0.517	0.193
	0.558	0.190
	0.599	0.122
	0.668	0.017
	0.696	0.171
	0.744	0.496
	0.799	0.301
	0.834	0.427
	0.876	0.598
	0.917	0.848
[4 3 4]	0.358	0.269
	0.401	0.313
	0.454	0.234
	0.517	0.164
	0.558	0.156
	0.599	0.091
	0.629	0.029
	0.697	0.073
	0.744	0.231
	0.790	0.345
	0.834	0.376
	0.876	0.464
[5 3 5]	0.401	0.242
	0.454	0.261
	0.517	0.214
	0.558	0.120
	0.599	0.071
	0.699	0.049
	0.744	0.193
	0.799	0.361
	0.834	0.480
[2 1 2]	0.517	0.247
	0.558	0.179
	0.599	0.066
	0.697	0.035
	0.744	0.262
	0.790	0.564
	0.834	0.721

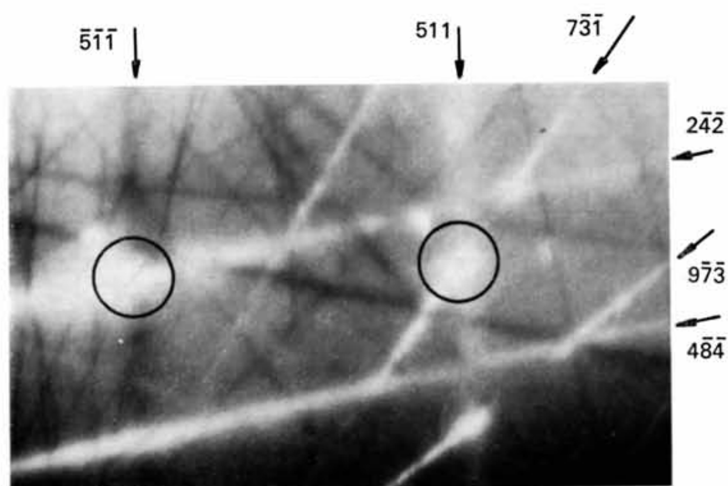

Fig. 1. Transmission Kikuchi pattern from natural spinel, $MgAl_2O_4$, showing split lines (encircled), enhanced and diminished line segments. Nominal voltage in all Figures: 100 kV.

Fig. 2. Transmission Kikuchi pattern showing split lines, enhanced and diminished line segments, displaced lines, *e.g.* $\pm 642'$.

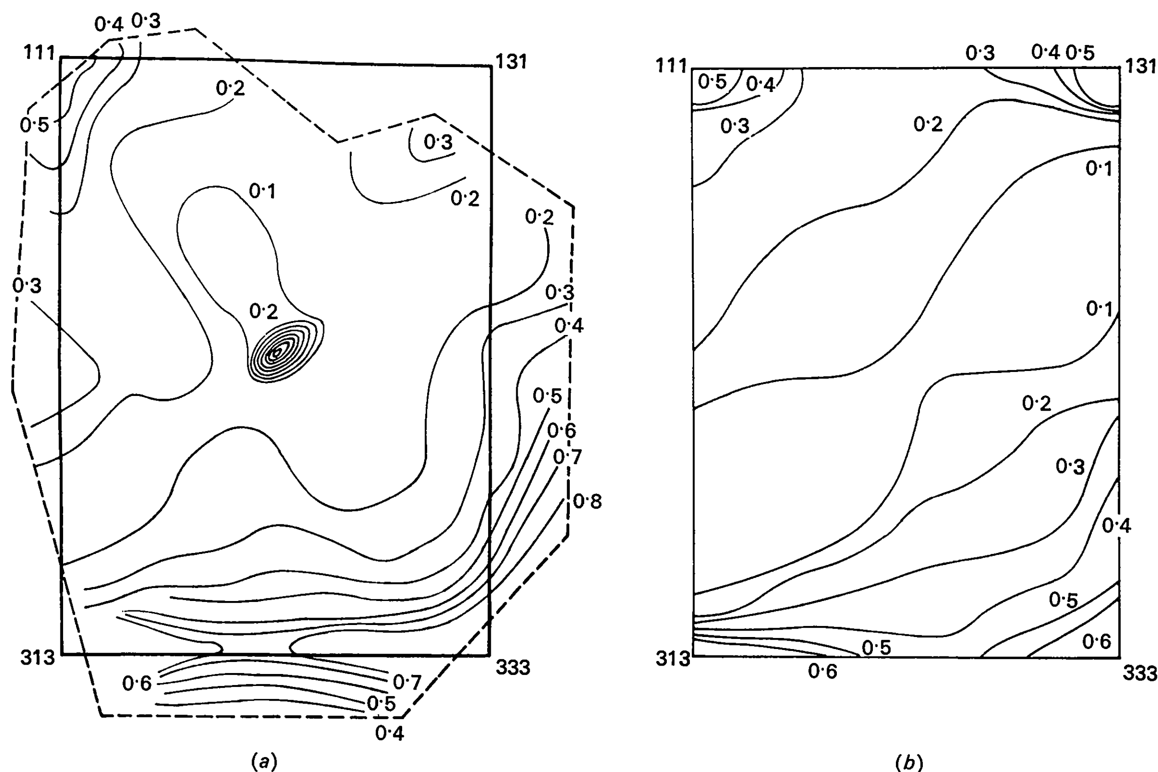

Fig. 4. Equi-intensity contour in the (Ī01) plane: (*a*) from measured intensities. Around relp (222) each succeeding contour line represents diffuse intensity higher by 0·1 than the preceding line. (*b*) from calculated first-order thermal scattering power.

of temperature, for which Hoerni & Wooster (1955) established the form of spikes in reciprocal space. The X-ray diffraction spikes of diamond have been attributed to defects and are entirely absent in some diamonds. Diffuse scattering of X-rays and electrons from $BaTiO_3$ single crystals was attributed by Harada, Watanabe, Kodera & Honjo (1965) to thermal diffuse scattering due to low-frequency transverse optic lattice waves, but Comes, Lambert & Guinier (1968) attributed it to a partially disordered structure.

In our measurements on silicon single crystals we did not find any scattering corresponding to spikes in diamonds. Compared with streaks given by $BaTiO_3$, diffuse streaks in silicon are wider, and wide streaks are characteristic for diffuse scattering of a really thermal origin.

The author would like to express his gratitude to Professor A. Guinier, who gave the initiative for this work and offered helpful advice. Thanks are also due to Mr D. Taupin and Mr Lj. Dacic for their help in the machine computations.

References

Banerjee, R. L. (1964). *C. R. Acad. Sci. Paris*, **258**, 5845.
Banerjee, R. L. (1967). *Bull. Soc. franç. Minér. Crist.* **90**, 130.
Brockhouse, B. N. & Iyengar, P. K. (1958). *Phys. Rev.* **111**, 747.
Comes, R., Lambert, M. & Guinier, A. (1968). *C. R. Acad. Sci. Paris*, **266**, 959.
Corbeau, J. (1963). Ph. D. Thesis, Paris.
Corbeau, J. (1964). *J. Phys.* **25**, 925.
Dolling, G. (1962). *Lattice Vibrations in Crystals with the Diamond Structure*. Paper presented to the IAEA Symposium on Inelastic Scattering of Neutrons in Solids and Liquids, Chalk River, Ontario (September 1962).
Freeman, A. J. (1959). *Acta Cryst.* **12**, 929.
Guinier, A. (1964). *Théorie et Technique de la Radiocristallographie*. 3rd ed. Paris: Dunod.
Harada, J., Watanabe, M., Kodera, S. & Honjo, G. (1965). *J. Phys. Soc. Japan*, **20**, 630.
Heidenreich, R. D. (1950). *Phys. Rev.* **77**, 271.
Hoerni, J. A. & Wooster, W. A. (1955). *Acta Cryst.* **8**, 187.
Honjo, G., Kodera, S. & Kitamura, N. (1964). *J. Phys. Soc. Japan*, **19**, 351.
Kodera, S., Kitamura, N. & Honjo, G. (1963). *J. Phys. Soc. Japan*, **18**, 317.
Komatsu, K. (1964). *J. Phys. Soc. Japan*, **19**, 1243.
Laval, J. (1954). *J. Phys. Radium*, **15**, 545 & 657.
McSkimin, H. J. (1953). *J. Appl. Phys.* **24**, 988.
Smith, H. M. J. (1948). *Trans. Roy. Soc.* A**241**, 105.
Renninger, M. (1937). *Z. Physik*, **106**, 141.